Reducing Jagged 1 and 2 levels prevents cerebral arteriovenous malformations in matrix Gla protein deficiency

Yucheng Yao[a,1], Jiayi Yao[a], Melina Radparvar[a], Ana M. Blazquez-Medela[a], Pierre J. Guihard[a], Medet Jumabay[a], and Kristina I. Boström[a,b,1]

[a]Division of Cardiology, David Geffen School of Medicine at UCLA and [b]Molecular Biology Institute, University of California, Los Angeles, CA 90095-1679

Edited by Kari Alitalo, University of Helsinki, Finland, and approved October 16, 2013 (received for review June 7, 2013)

Cerebral arteriovenous malformations (AVMs) are common vascular malformations, which may result in hemorrhagic strokes and neurological deficits. Bone morphogenetic protein (BMP) and Notch signaling are both involved in the development of cerebral AVMs, but the cross-talk between the two signaling pathways is poorly understood. Here, we show that deficiency of matrix Gla protein (MGP), a BMP inhibitor, causes induction of Notch ligands, dysregulation of endothelial differentiation, and the development of cerebral AVMs in MGP null ($Mgp^{-/-}$) mice. Increased BMP activity due to the lack of MGP induces expression of the activin receptor-like kinase 1, a BMP type I receptor, in cerebrovascular endothelium. Subsequent activation of activin receptor-like kinase 1 enhances expression of Notch ligands Jagged 1 and 2, which increases Notch activity and alters the expression of Ephrin B2 and Ephrin receptor B4, arterial and venous endothelial markers, respectively. Reducing the expression of Jagged 1 and 2 in the $Mgp^{-/-}$ mice by crossing them with Jagged 1 or 2 deficient mice reduces Notch activity, normalizes endothelial differentiation, and prevents cerebral AVMs, but not pulmonary or renal AVMs. Our results suggest that Notch signaling mediates and can modulate changes in BMP signaling that lead to cerebral AVMs.

angiogenesis | shunt | animal model | hereditary hemorrhagic telangiectasia | brain circulation

Cerebral arteriovenous malformations (AVMs) are abnormal vascular networks that form direct connections between arteries and veins, thereby short circuiting the cerebral capillary system. Due to the elevated blood pressure in these abnormal connections, vessels may ultimately rupture and result in hemorrhagic strokes (1–3). The development of cerebral AVMs has been shown to involve bone morphogenetic protein (BMP) and Notch signaling, both essential pathways in vascular formation (4, 5). Mutations in the genes for activin-like kinase receptor 1 (ALK1), a BMP type I receptor, and Endoglin, a coreceptor of ALK1, cause hereditary hemorrhagic telangiectasia (HHT) characterized by the presence of AVMs in multiple organs including the brain (6–9). Enhanced endothelial Notch signaling, as mediated by constitutively active Notch4, also promotes the formation of brain AVMs, whereas normalization of Notch4 activity results in regression of arteriovenous (AV) shunts (10, 11).

We have previously shown that BMP-4 and -7 induce expression of ALK1 in endothelial cells (ECs) (12, 13). In turn, activation of ALK1 by its ligand BMP-9 induces expression of matrix Gla protein (MGP), an inhibitor of BMP-2, -4 and -7 (12-15), which is highly expressed in brain, lungs, and kidneys (13, 16). MGP provides negative feedback inhibition for BMP-4 and -7 (13, 17), which limits the ALK1 induction. Gene deletion of MGP in mice results in excess ALK1 activation and severe AVMs in lungs and kidneys (13). However, it has not yet been shown whether AVMs also form in the brain of MGP null ($Mgp^{-/-}$) mice.

Connections between BMP-9/ALK1 and Notch signaling have been reported. Larrivée et al. reported that BMP-9/ALK1 activation induces the expression of Notch ligands and targets in vascular ECs (18), suggesting that Notch signaling acts on the vasculature downstream of BMP-9/ALK1. Even so, it is not clear how ALK1 signaling affects Notch signaling and vice versa during the formation of AVMs.

Here, we report that the formation of cerebral AVMs occurs in $Mgp^{-/-}$ mice, but is prevented by decreasing the expression of the Notch ligands Jagged 1 and 2, which compensates for the excess ALK1 activation in these mice. The results suggest that maintaining the balance between BMP and Notch signaling is essential to avoid AVMs.

Results

Lack of MGP Causes Cerebral AVMs. To determine if AVMs are present in the brain of $Mgp^{-/-}$ mice, we examined the cerebral vasculature of $Mgp^{-/-}$, $Mgp^{+/-}$, and wild type ($Mgp^{+/+}$) mice at 4 wk of age. The results revealed enlarged vessels and direct connections between arteries and veins characteristic of cerebral AVMs in the $Mgp^{-/-}$ mice, but not in the $Mgp^{+/-}$ or $Mgp^{+/+}$ mice, as shown by microcomputed tomography (micro-CT) imaging. Images from the 3D analysis are shown in Fig. 1*A* (Movies S1–S3 show full reconstructions). Analysis of the vessel radius by micro-CT showed an increase in the frequency of vessels of all radii between 10 and 100 μm in the $Mgp^{-/-}$ mice (Fig. 1*C*). Vascular casting and immunostaining with antibodies to CD31, an endothelial marker, further confirmed the presence of abnormal and

Significance

Cerebral arteriovenous malformations (AVMs) are common vascular abnormalities that may lead to strokes. Signaling by bone morphogenetic proteins (BMPs) and Notch play important roles in the formation of cerebral AVMs, but the cross-talk between the pathways is poorly understood. We report that gene deletion of matrix Gla protein (MGP), a BMP inhibitor, causes cerebral AVMs in mice by activating activin receptor-like kinase 1, a BMP receptor. This activation enhances Notch activity and disrupts endothelial cell differentiation by inducing the Notch ligands Jagged 1 and 2. Reducing Jagged 1 and 2 expression prevents the disruption in differentiation and AVM formation. The findings suggest that MGP maintains the balance between BMP and Notch signaling and promotes a normal brain vasculature.

Author contributions: Y.Y., J.Y., M.R., A.M.B.-M., P.J.G., M.J., and K.I.B. designed research; Y.Y., J.Y., M.R., A.M.B.-M., P.J.G., and M.J. performed research; Y.Y. and K.I.B. contributed new reagents/analytic tools; Y.Y. and K.I.B. analyzed data; and Y.Y. and K.I.B. wrote the paper.

The authors declare no conflict of interest.

This article is a PNAS Direct Submission.

[1]To whom correspondence may be addressed. E-mail: yyao@mednet.ucla.edu or kbostrom@mednet.ucla.edu.

This article contains supporting information online at www.pnas.org/lookup/suppl/doi:10.1073/pnas.1310905110/-/DCSupplemental.

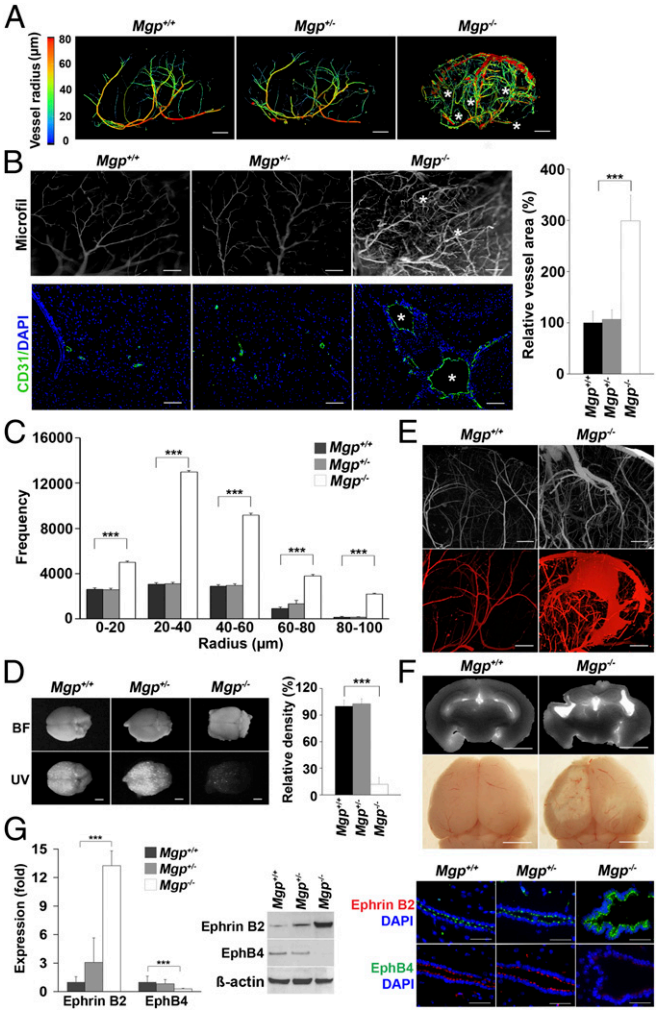

Fig. 1. MGP deficiency causes cerebral AVMs. (*A*) Micro-CT images of the cerebral vasculature with colors reflecting the vessel radii from wild-type ($Mgp^{+/+}$), $Mgp^{+/-}$, and $Mgp^{-/-}$ mice ($n = 3$). Asterisks represent arteriovenous (AV) connections. Movies S1–S3 show full 3D reconstructions of the cerebral vasculatures. (*B*) Presence of AV connections and enlarged vessels in the cerebral vasculature of $Mgp^{-/-}$ mice, as shown by vascular casting (MICROFIL) (*Upper Left*) ($n = 3$) and immunostaining for the endothelial marker CD31 (*Lower Left*) ($n = 3$). Asterisks represent AV shunts. Relative vessel area of the cerebral vasculature in $Mgp^{+/+}$, $Mgp^{+/-}$, and $Mgp^{-/-}$ mice ($n = 8$) (*Right*). (*C*) Radius analysis of the cerebral vasculature in $Mgp^{+/+}$, $Mgp^{+/-}$, and $Mgp^{-/-}$ mice ($n = 5$). (*D*) AV shunting in $Mgp^{-/-}$ mice as demonstrated by UV-fluorescent microsphere passage (*Lower Left*); (BF, bright field) (*Upper Left*). Relative density of retained fluorescence in the brains of $Mgp^{+/+}$, $Mgp^{+/-}$, and $Mgp^{-/-}$ mice after microsphere injection ($n = 8$) (*Right*). (*E*) Nidus of cerebral AVMs in $Mgp^{-/-}$ mice as shown by vascular casting (*Upper*). Evidence of fresh cerebral hemorrhage in $Mgp^{-/-}$ mice as visualized by micro-CT (*Lower*). (*F*) Evidence of old cerebral injury in $Mgp^{-/-}$ mice as shown by micro-CT (*Upper*) and dissection microscopy (*Lower*). (*G*) Expression of Ephrin B2 and Eph B4 in brain tissue from $Mgp^{+/+}$, $Mgp^{+/-}$, and $Mgp^{-/-}$ mice as determined by real-time PCR, immunoblotting, and immunostaining. β-Actin was used as control for immunoblotting. ***$P < 0.0001$. [Scale bar, 1 mm (*A* and *D–F*); 100 μm (*B* and *G*).]

enlarged vessels in the brain of $Mgp^{-/-}$ mice (Fig. 1*B*). Furthermore, injection of fluorescent microspheres that are normally retained in the brain tissue, easily passed through the $Mgp^{-/-}$ brains, which supported the presence of AVMs (Fig. 1*D*). Niduses of abnormally connecting vessels and signs of fresh hemorrhage (Fig. 1*E*) as well as old injury (Fig. 1*F*) were demonstrated by micro-CT and visualization through a dissection microscope. Findings consistent with AVMs were found in 100% of the studied $Mgp^{-/-}$ mice. The arterial oxygen saturation in $Mgp^{-/-}$ and Mgp^{++} mice was similar (Fig. S1) and therefore unlikely to be the cause of the vascular abnormalities.

We further examined Ephrin B2 and Ephrin receptor B4 (EphB4), markers for arterial and venous ECs, respectively. The expression of Ephrin B2 increased significantly in the brains of $Mgp^{-/-}$ mice, as determined by real-time PCR and immunoblotting (Fig. 1*G*, *Left*), whereas the expression of Eph B4 decreased (Fig. 1*G*, *Left*). Similarly, immunostaining revealed enhanced Ephrin B2 in the endothelium of the enlarged vessels in the $Mgp^{-/-}$ mice (Fig. 1*G*, *Right*), whereas Eph B4 was reduced (Fig. 1*G*, *Right*). No changes were detected in the brains of $Mgp^{+/-}$ compared with the $Mgp^{+/+}$ mice. Thus, cerebral AVMs occurred in the $Mgp^{-/-}$ mice and were associated with significant changes in the differentiation of arterial and venous ECs.

Activated BMP Signaling Alters Expression of ALK1, Jagged 1 and 2, Ephrin B2, and Eph B4 in the Cerebrovascular Endothelium of $Mgp^{-/-}$ Mice. To determine the effect of loss of MGP on BMP signaling, we compared the levels of activated, phosphorylated (p)SMAD1/5/8 in the brains of the different mice. We found that pSMAD1/5/8 was strongly enhanced in the $Mgp^{-/-}$ mice, as determined by immunoblotting (Fig. 2*A*, *Upper*). Furthermore, immunostaining showed colocalization of pSMAD1/5/8 with CD31 (Fig. 2*A*,

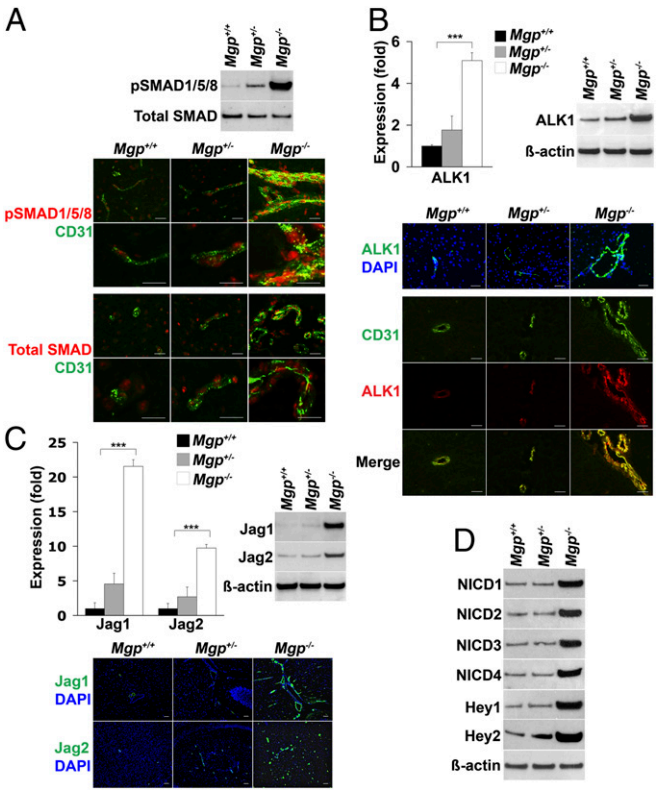

Fig. 2. Excess ALK1 signaling induces expression of Notch ligands. (*A*) pSMAD1/5/8 in brain tissue from $Mgp^{+/+}$, $Mgp^{+/-}$, and $Mgp^{-/-}$ mice, as determined by immunoblotting (*Upper*) and immunostaining (*Lower*) and compared with total SMAD and the endothelial cell marker CD31 ($n = 3$). (*B*) Expression of ALK1 in the brain tissue from $Mgp^{+/+}$, $Mgp^{+/-}$, and $Mgp^{-/-}$ mice as determined by real-time PCR, immunoblotting, and immunostaining. ALK1 (red) colocalized with CD31 (green). (*C*) Jagged 1 (Jag1) and Jagged 2 (Jag2) in the brain tissue from $Mgp^{+/+}$, $Mgp^{+/-}$, and $Mgp^{-/-}$ mice as determined by real-time PCR, immunoblotting, and immunostaining. (*D*) Notch intracellular domains (NICDs) of Notch1–4 and expression of Hey1 and Hey2 in the brain tissue from $Mgp^{+/+}$, $Mgp^{+/-}$, and $Mgp^{-/-}$ mice as determined by immunoblotting. β-Actin was used as control. ***$P < 0.0001$. (Scale bar, 100 μm.)

Lower), as well as with smooth muscle cell markers (Fig. S2). Because BMP activity enhances endothelial ALK1 expression in lungs and kidneys (13), we also determined the expression of ALK1 in the MGP-deficient brains. The results showed that ALK1 was strongly induced in the brains of *Mgp*$^{-/-}$ mice where it colocalized with CD31 in ECs, as determined by real-time PCR, immunoblotting, and immunostaining (Fig. 2*B*). ALK1/BMP-9 signaling has previously been shown to induce expression of the Notch ligand Jagged 1 in human umbilical vein ECs (18), as well as the Notch targets Ephrin B2 and Eph B4 (19). Therefore, we examined the expression of the Notch ligands (Jagged 1 and 2, Delta-like (Dll)1, -3, and -4), Notch receptor 1–4, and the downstream target genes Hey1 and -2 in the brains of *Mgp*$^{-/-}$ mice. The expression of Jagged 1 and 2, as well as that of Hey1 and -2 increased significantly in the *Mgp*$^{-/-}$ mice, as determined by real-time PCR and immunoblotting (Fig. 2 *C*, *Upper* and *D*, *Lower*). The expression of other Notch ligands and receptors showed no significant change (Fig. S3). Immunostaining revealed that expression of Jagged 1 and 2 was enhanced in the endothelium of the enlarged vessels in the *Mgp*$^{-/-}$ mice (Fig. 2*C*, *Lower*). The Notch intracellular domains (NICDs) of Notch 1–4 were increased in the brains of *Mgp*$^{-/-}$ mice, as determined by immunoblotting (Fig. 2*D*). Thus, the lack of MGP in the brain increased BMP and Notch activity and expression of ALK1, Jagged 1 and 2, and Hey1 and -2.

Activated ALK1 Induces Expression of Jagged 1 and 2, Which Increases Ephrin B2 and Decreases Eph B4 in Human Brain Microvascular Endothelial Cells. To explore if activated ALK1 induced the expression of Jagged 1 and 2, Notch activity, and the expression of downstream targets in cerebrovascular ECs, we treated human brain microvascular endothelial cells (HBMECs) with BMP-9, a ligand of ALK1, for 20–24 h (20). The results showed a strong induction of Jagged 1 and 2, Ephrin B2, and Hey1 and -2, and increases in the levels of pSMAD1/5/8 and all of the NICDs, whereas the expression of Eph B4 decreased, as determined by immunoblotting (Fig. 3*A*), suggesting that the Notch activity is regulated downstream of ALK1. Because ALK1 is induced in MGP deficiency (13), we next depleted MGP in HBMECs using siRNA as verified by immunocytochemistry (Fig. S4). We examined the expression of Jagged 1 and 2, Ephrin B2 and Eph B4, as well as the Notch activity. The cells were lysed 24 h after siRNA transfection. The results similarly showed a strong induction of Jagged 1 and 2, Ephrin B2, and Hey1 and -2, and increases in the levels of pSMAD1/5/8 and the NICDs, but a reduction of Eph B4 expression, as determined by immunoblotting (Fig. 3*B*). We also depleted ALK1 and SMAD1 using siRNA, which abolished the induction of Jagged 1 and 2, Ephrin B2, and Hey1 and -2, the increases in pSMAD1/5/8 and the NICDs, and the reduction of Eph B4 (Fig. 3 *B* and *E*), further supporting that the changes occurred through ALK1 activation.

We then examined the expression of Jagged 1 and 2, Ephrin B2, Eph B4, and Hey1 and -2, and the levels of pSMAD1/5/8 and the NICDs after depletion of MGP and/or ALK1, with or without BMP-9 treatment. The treatment was initiated 12 h after siRNA transfection and the cells were lysed after 24 h of treatment. Depletion of MGP together with BMP-9 treatment synergistically increased the expression of Jagged 1 and 2, Ephrin B2, and Hey1 and -2, and the levels of pSMAD1/5/8 and NICDs, but reduced the expression of Eph B4, as determined by immunoblotting (Fig. 3*C*). However, ALK1 depletion limited these changes (Fig. 3*C*), supporting that ALK1 mediates the induction of the Notch ligands and their downstream targets. Furthermore, we examined the expression of Ephrin B2, Eph B4, Hey1 and -2, and the levels of the NICDs after depletion of MGP and Jagged 1 and 2 together with BMP-9 treatment. The results showed that the changes in Ephrin B2, Eph B4, Hey1 and -2, and NICDs that were due to MGP depletion largely normalized after depletion of

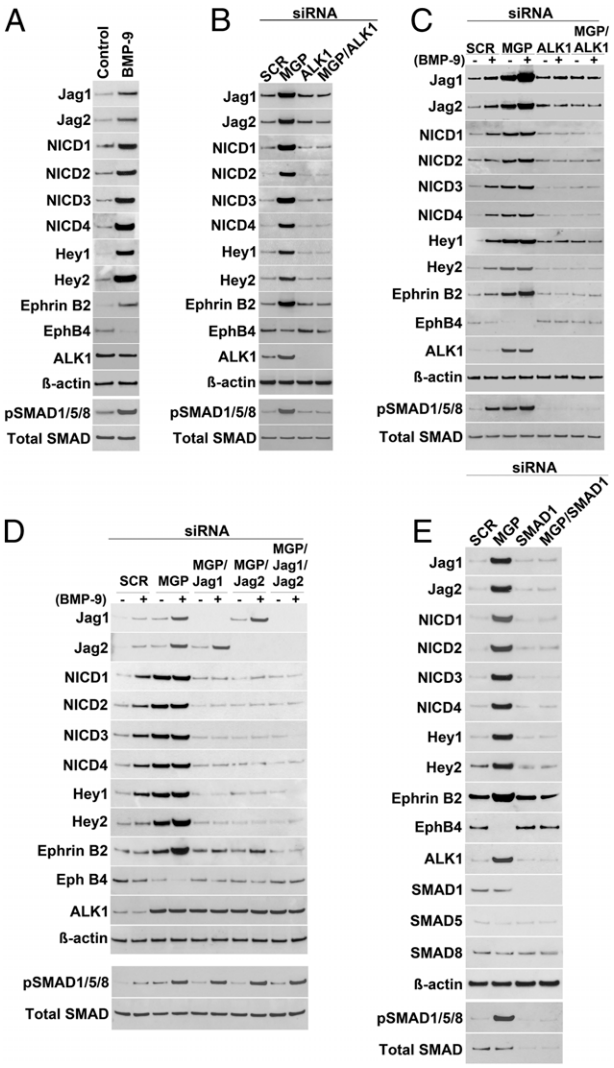

Fig. 3. ALK1 signaling enhances Notch ligands and Notch targets in human brain microvascular endothelial cells (HBMECs). (*A–D*) Expression of Jagged 1 (Jag1), Jagged 2 (Jag2), Hey1, Hey2, Ephrin B2, Eph B4, ALK1, and levels of Notch intracellular domains (NICDs) of Notch1–4, pSMAD1/5/8, and total SMAD in HBMECs by immunoblotting after (*A*) treatment of BMP-9; (*B*) transfection with siRNA to MGP, ALK1, or MGP and ALK1; (*C*) transfection with siRNA to MGP, ALK1, or MGP and ALK1, combined with treatment with (+) or without (–) BMP-9; and (*D*) transfection with siRNA to MGP, MGP and Jagged 1, MGP and Jagged 2, or MGP and Jagged 1/Jagged 2, combined with treatment with (+) or without (–) BMP-9. (*E*) Expression of Jagged 1, Jagged 2, Hey1, Hey2, Ephrin B2, Eph B4, ALK1, SMAD1, SMAD5, and SMAD8, and levels of NICDs of Notch1–4, pSMAD1/5/8, and total SMAD in HBMECs after transfection with siRNA to MGP, SMAD1, or MGP and SMAD1, as determined by immunoblotting. Scrambled siRNA (SCR) was used as control in *B–E*. β-Actin was used as control for immunoblotting.

Jagged 1 and/or 2, as determined by immunoblotting and immunostaining (Fig. 3*D* and Fig. S5). Depletion of Jagged 1 and 2 did not significantly alter the pSMAD1/5/8 levels. These results suggest that a reduction in Jagged 1 and/or 2 might limit the disruption caused by the enhanced ALK1 activation in MGP-deficient mice.

Reducing Levels of Jagged 1 or 2 Limited Notch Activity and Prevented Cerebral AVMs in *Mgp*$^{-/-}$ Mice. Based on the in vitro results, we hypothesized that limiting expression of Jagged 1 or 2 in *Mgp*$^{-/-}$ mice would improve the cerebral AVMs. To test this hypothesis, we crossed mice heterozygous for deletion of the *Jagged 1* (*Jag1*$^{+/-}$)

or *Jagged 2* ($Jag2^{+/-}$) gene with the $Mgp^{-/-}$ mice, respectively, and examined the cerebral vasculature of $Mgp^{-/-}Jag1^{+/-}$ and $Mgp^{-/-}Jag2^{+/-}$ mice by micro-CT, vascular casting, injection of microspheres, and expression of arterial and venous EC markers. The micro-CT showed that the cerebral vasculature in the $Mgp^{-/-}Jag1^{+/-}$ and $Mgp^{-/-}Jag2^{+/-}$ mice was indistinguishable from the $Mgp^{+/+}$ mice (Fig. 4*A*; Movies S4–S9 show full reconstructions). The frequency of vessels of different radii by micro-CT was similar (Fig. 4*B*) and showed together with the vascular casting (Fig. 4*C*) that the decreased Jagged expression had prevented the abnormal AV connections seen in the $Mgp^{-/-}$ mice. As expected, the functional assays showed that injected microspheres were retained in the brains of $Mgp^{-/-}Jag1^{+/-}$ and $Mgp^{-/-}Jag2^{+/-}$ mice (Fig. 4*D*). Furthermore, the increases in Ephrin B2, Hey1 and -2, and the NCIDs, as well as the reduction of Eph B4 were eliminated in the brains of $Mgp^{-/-}Jag1^{+/-}$ and $Mgp^{-/-}Jag2^{+/-}$ mice, as determined by immunoblotting (Fig. 5*A*). Expression of ALK1 and pSMAD1/5/8 levels did not change when the Jagged expression was reduced (Fig. 5*B*), supporting that Jagged 1 and 2 act downstream of ALK1.

To explore the mechanisms of AVMs in different organs, we compared the expression of the vascular endothelial growth factor (VEGF) and Jagged 1 and 2 in the lungs, kidneys, and brains of $Mgp^{-/-}$ mice (Fig. 6*A*). The results showed that the VEGF expression increased in the lungs and kidneys, but not in the brain of $Mgp^{-/-}$ mice. On the other hand, Jagged 1 and 2 increased in the brain of $Mgp^{-/-}$ mice, but not in the lungs and kidneys, suggesting that Jagged 1 and 2 have less of a role in pulmonary and renal AVMs. We examined the functionality of AVMs in lungs and kidneys of $Mgp^{-/-}Jag1^{+/-}$ and $Mgp^{-/-}Jag2^{+/-}$ mice by injecting UV microspheres. The results showed that the microspheres were not retained in the lungs or kidneys of the $Mgp^{-/-}Jag1^{+/-}$ and $Mgp^{-/-}Jag2^{+/-}$ mice (Fig. 6 *B* and *C* and Fig. S6), suggesting that the decreased Jagged 1 and 2 levels had not prevented the formation of AVMs.

Together, these experiments show that the mechanism of cerebral AVMs differs from that of AVMs in lung and kidneys in $Mgp^{-/-}$ mice, and that a reduction of Jagged 1 or 2 prevents the effects of the increased ALK1 signaling in $Mgp^{-/-}$ mice and the development of cerebral AVMs.

Discussion

Although both ALK1 and Notch signaling are known to affect the development of AVMs, connections between the two systems in AVMs are still unclear. Our findings suggest that MGP deficiency causes cerebral AVMs through an imbalance in the sequential activation of ALK1 and Notch signaling in the endothelium. Specifically, the lack of MGP enhances expression of ALK1, which after activation induces excess Jagged 1 and 2, and disrupts EC specification by altering expression of Ephrin B2 and Eph B4. The formation of cerebral AVMs in $Mgp^{-/-}$ mice was prevented by a reduction in Jagged 1 or 2 expression, which offset the ALK1 activation. Even though we cannot be certain that all abnormalities are corrected by the decrease in Notch signaling, it suggests that the critical step(s) in AVM formation is located downstream of Jagged 1 and 2. Interestingly, the same modulation did not prevent pulmonary and renal AVMs, suggesting that Notch signaling may have antiangiogenic effects in these organs, as previously suggested by Larrivée et al. (18). Other investigators have reported the involvement of additional Notch components in the formation of AVMs, including Dll4, Notch3, and Notch4 (10, 21–23), but it remains unclear if these components are regulated by ALK1 activation.

AVMs also occur in patients and mice with HHT2, where the ALK1 receptor is mutated and the ALK1 expression is reduced (6, 7, 24). The incidence of AVMs in HHT2 is about 25% (25). Although decreased ALK1 results in decreased MGP (26), it is not clear if the low MGP is the cause of the AVMs or if there are differences in the AVMs that are formed when ALK1 activity is low versus high. It is possible that the balance between ALK1 and Notch signaling, rather than the absolute levels of expression, determines if AVMs are formed, in which case a variety of disruptions in ALK1 and/or Notch could lead to the same phenotype.

Previous studies have indicated that Notch activity promotes arterial EC specification while repressing venous EC specification (19). Gene deletion of Dll4 and Hey1/Hey2 in mice leads to

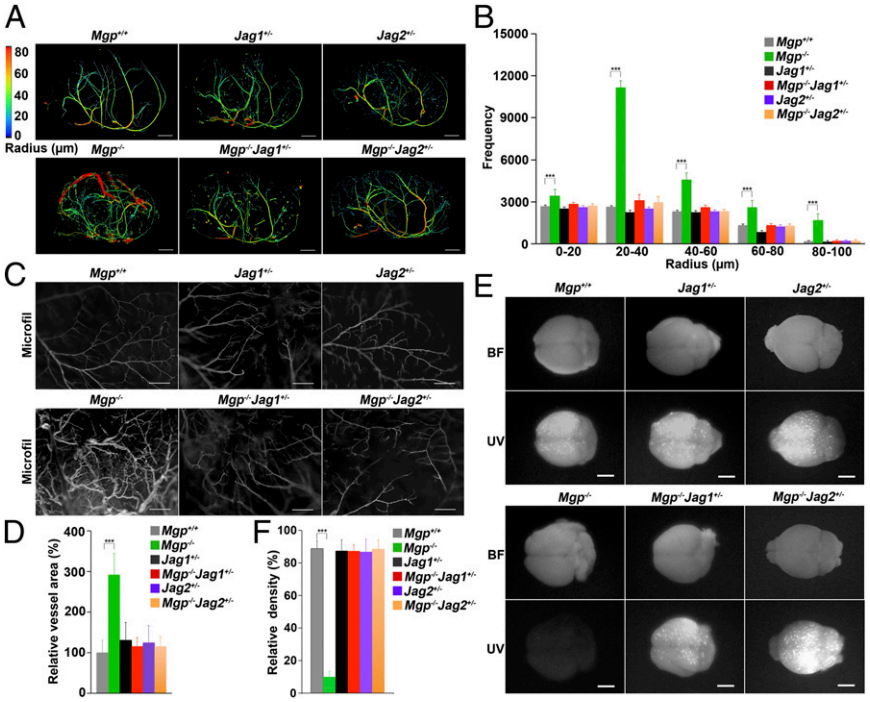

Fig. 4. Reduced expression of Jagged 1 or Jagged 2 prevents cerebral AVMs in $Mgp^{-/-}$ mice. (*A*) Micro-CT images of the cerebral vasculature with colors reflecting the vessel radii from wild-type ($Mgp^{+/+}$), $Jag1^{+/-}$, $Jag2^{+/-}$, $Mgp^{-/-}$, $Mgp^{-/-}Jag1^{+/-}$, and $Mgp^{-/-}Jag2^{+/-}$ mice (n = 3). Movies S4–S9 show full 3D reconstructions of the cerebral vasculatures. (*B*) Radius analysis of the cerebral vasculature of $Mgp^{+/+}$, $Jag1^{+/-}$, $Jag2^{+/-}$, $Mgp^{-/-}$, $Mgp^{-/-}Jag1^{+/-}$, and $Mgp^{-/-}Jag2^{+/-}$ mice (n = 5). (*C*) Absence of AV connections in the cerebral vasculature of $Mgp^{-/-}Jag1^{+/-}$ and $Mgp^{-/-}Jag2^{+/-}$ mice, as shown by vascular casting (MICROFIL) (n = 3). (*D*) Relative vessel area in the cerebral vasculature of $Mgp^{+/+}$, $Jag1^{+/-}$, $Jag2^{+/-}$, $Mgp^{-/-}$, $Mgp^{-/-}Jag1^{+/-}$, and $Mgp^{-/-}Jag2^{+/-}$ mice (n = 8). (*E*) Absence of AV shunting in the cerebral vasculature of $Mgp^{-/-}Jag1^{+/-}$ and $Mgp^{-/-}Jag2^{+/-}$ mice, as demonstrated by UV-fluorescent microsphere passage (BF, bright field). The microspheres were retained in all brains except those of $Mgp^{-/-}$ mice (n = 3). (*F*) Relative density of retained fluorescence after microsphere injection in the brains shown in *E* (n = 8). ***$P < 0.0001$. [Scale bar, 1 mm (*A* and *E*); 100 μm (*B*).]

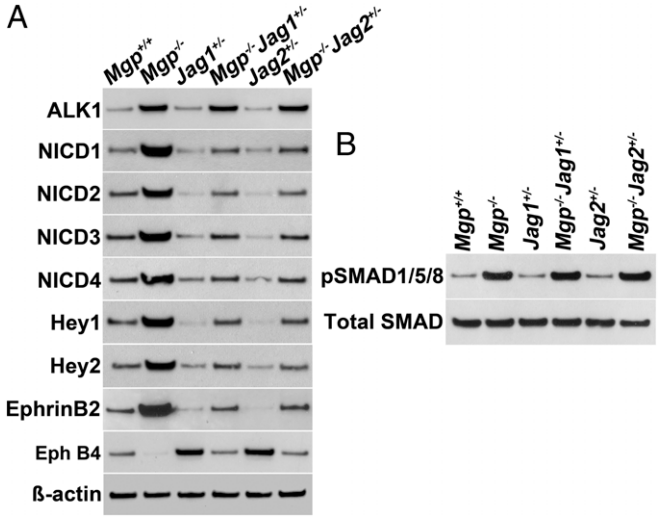

Fig. 5. Levels of ALK1, NICDs, Notch targets, and pSMAD1/5/8 in the brains of $Mgp^{-/-}$ mice with reduced expression of Jagged 1 or Jagged 2. (*A*) Expression of ALK1, Hey1, Hey2, Ephrin B2 and Eph B4, and levels of NICDs of Notch1–4 in the brain tissue of $Mgp^{+/+}$, $Jag1^{+/-}$, $Jag2^{+/-}$, $Mgp^{-/-}$, $Mgp^{-/-}Jag1^{+/-}$, and $Mgp^{-/-}Jag2^{+/-}$ mice, as determined by immunoblotting ($n = 3$). β-Actin was used as control. (*B*) PSMAD1/5/8 and total SMAD in the brains of same mice as in *A*.

reduce expression of the arterial marker Ephrin B2 (22, 27, 28) and enhanced expression of the venous marker Eph B4 (29). Constitutively active Notch4 increases expression of Ephrin B2 in the brain vasculature and causes cerebral AVMs (10), and loss of function of Ephrin B2 and Eph B4 affects vascular remodeling and intercalation of arterial and venous vasculature (30). We showed that an increase in Ephrin B2 and a decrease in Eph B4 are associated with AVMs in the $Mgp^{-/-}$ mice, which is consistent with the previous studies. It suggests that an imbalance favoring the arterial EC differentiation is important in the formation of AVMs, although it is not clear why.

The functionality of MGP depends on correct gamma-carboxylation of glutamate residues in the MGP protein (14), and non–gamma-carboxylated MGP has been observed in the vasculature after warfarin treatment (31). If there is sufficient inhibition of the gamma-carboxylation, it could increase the risk of AVM formation, although this has not been investigated.

In summary, this study shows that modulation of Notch signaling can compensate for, and largely prevent, cerebrovascular malformations due to abnormal ALK1 signaling.

Methods

Animals. $Mgp^{+/-}$ mice on a C57BL/6J background were obtained from Cecilia Giachelli (University of Washington, Seattle), with the permission of Gerard Karsenty (Columbia University, NY). $Jag1^{+/-}$ and $Jag2^{+/-}$ mice were obtained from the Jackson Laboratory. Genotypes were confirmed by PCR (32–34), and experiments were performed with generations F4–F6. Littermates were used as wild-type controls. All mice were fed a standard chow diet (Diet 8604; Harlan Teklad Laboratory), and mice were used for experiments at 4 wk of age. The investigation conformed to the Guide for the Care and Use of Laboratory Animals published by the National Institutes of Health (NIH Publications No. 85–23, revised 1996) and had been reviewed and approved by the Institutional Review Board of the University of California, Los Angeles.

Micro-CT Imaging. Micro-CT was performed by Numira Biosciences. The perfusion with the MICROFIL compound and the preparation of the specimens were performed as previously described in detail (13). All of the samples were scanned on a high-resolution, volumetric micro-CT scanner (μCT 40; ScanCo Medical) at Numira Biosciences. The image data were acquired with the following parameters: 10-μm isotropic voxel resolution; 200-ms exposure time; 2,000 views; and five frames per view. The micro-CT generated digital imaging and communications in medicine (DICOM) files were used to analyze the samples and to create volume renderings of the regions of interest. The raw data files were viewed using the MicroView 3-D volume viewer and analysis tool (GE Healthcare) and AltaViewer Software (Numira). Additionally, images of the sample were generated using SCIRun (Scientific Computing and Imaging Institute, University of Utah, Salt Lake City; www.sci.utah.edu/cibc/software/106-scirun.html).

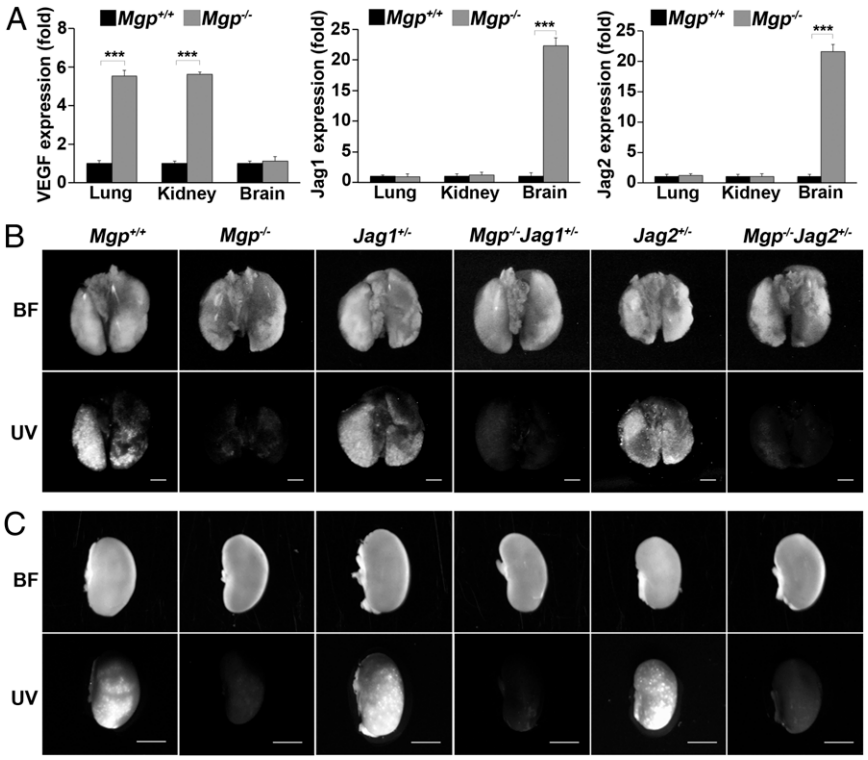

Fig. 6. Reduced Jagged 1 and 2 did not prevent AVMs in the lungs and kidneys of $Mgp^{-/-}$ mice. (*A*) Expression of VEGF, Jagged 1 (Jag1) and Jagged 2 (Jag2) in the lungs, kidneys, and brains of $Mgp^{+/+}$ and $Mgp^{-/-}$ mice. (*B* and *C*) AV shunting in lungs and kidneys of $Mgp^{-/-}$, $Mgp^{-/-}Jag1^{+/-}$, and $Mgp^{-/-}Jag2^{+/-}$ mice as demonstrated by UV-fluorescent microsphere passage (BF, bright field). The microspheres were not retained in the lungs and kidneys of $Mgp^{-/-}$, $Mgp^{-/-}Jag1^{+/-}$, or $Mgp^{-/-}Jag2^{+/-}$ mice (*Upper*) ($n = 6$). ***$P <$ 0.0001. (Scale bar, 2 mm.)

Vascular Casting. Casting of the cerebral vasculature was performed after perfusion with the MICROFIL compound as described (13).

Vascular Shunting. Fifteen-micrometer fluorescent microspheres (Invitrogen) were injected into the left ventricle immediately after sacrificing the mice, and the tissues were examined and photographed under UV light.

Tissue Culture and siRNA Transfections. HBMECs were obtained from ScienCell Research Laboratories and cultured as per the manufacturer's protocol. For treatment, BMP-9 (10 ng/mL) (R&D Systems) was added as indicated in *Results*. Transient transfections of HBMECs with siRNA (Silencer predesigned siRNA; Applied Biosystem) were optimized and performed as previously described (13). Compared with unrelated control siRNA and scrambled siRNA, the selected siRNAs resulted in a 90–95% decrease in mRNA and protein levels, as determined by real-time PCR and immunoblotting (or immunocytochemistry for MGP), respectively. Silencer predesigned siRNAs were obtained for MGP, ALK1, SMAD1, Jagged 1, and Jagged 2. Incubation with BMP-9 was initiated 3 h after transfection and after removal of Lipofectamine 2000.

RNA Analysis. Real-time PCR analysis was performed as previously described (17). GAPDH was used as a control gene. Primers and probes for ALK1, Jagged 1, Jagged 2, Ephrin B2, Eph B4, Notch1–4, and Hey1 and -2 were obtained from Applied Biosystems as part of TaqMan gene expression assays.

Immunoblotting. Immunoblotting was performed as previously described (35). Equal amounts of cellular protein were used. Blots were incubated with specific antibodies to pSMAD1/5/8 and SMAD1 (400 ng/mL; Cell Signaling Technology); SMAD5 (200 ng/mL; Abcam); SMAD8 (200 ng/mL; R&D Systems); total SMAD and Ephrin B2 (both 400 ng/mL; Santa Cruz Biotechnology), Eph B4 (200 ng/mL; Abcam), Jagged 1 and Jagged 2 (both 100 ng/mL; Cell Signaling Technology), NICD for Notch1 and -3 (100 ng/mL; Cell Signaling Technology), NICD for Notch2 and -4 (200 ng/mL; Millipore), and Hey1 and Hey2 (200 ng/mL; Millipore). β-Actin (1:5,000 dilution; Sigma-Aldrich) was used as loading control.

Immunostaining. Tissue sections were fixed, processed, and stained as previously described (35). Immunofluorescence was performed as previously described in detail (36, 37). Cultured cells were grown in chamber slides and fixed in 4% (wt/vol) paraformaldehyde for 30 min, permeabilized with 0.1% Triton X-100, blocked with 1% goat serum and 1% BSA in TBS, and stained using the same protocol as for the tissues. We used specific antibodies for pSMAD1/5/8, total SMAD, ALK1 (all from Santa Cruz Biotechnology), Jagged 1 and Jagged 2 (both Cell Signaling Technology), Ephrin B2 (Santa Cruz Biotechnology), and Eph B4 (Abcam). The nuclei were visualized with 4′,6-diamidino-2-phenylindole (DAPI; Sigma-Aldrich).

Statistics. Data were analyzed for statistical significance by ANOVA with post hoc Tukey's analysis. The analyses were performed using GraphPad Instat, version 3.0 (GraphPad Software). *P* values of less than 0.05 were considered significant. All experiments were repeated a minimum of three times.

ACKNOWLEDGMENTS. Funding for this work was provided in part by National Institutes of Health Grants NS79353, HL30568, HL81397, and DP3 DK094311, and the American Heart Association.

1. Friedlander RM (2007) Clinical practice. Arteriovenous malformations of the brain. *N Engl J Med* 356(26):2704–2712.
2. Al-Shahi R, et al.; Scottish Intracranial Vascular Malformation Study Collaborators (2003) Prospective, population-based detection of intracranial vascular malformations in adults: The Scottish Intracranial Vascular Malformation Study (SIVMS). *Stroke* 34(5): 1163–1169.
3. Leblanc GG, Golanov E, Awad IA, Young WL; Biology of Vascular Malformations of the Brain NINDS Workshop Collaborators (2009) Biology of vascular malformations of the brain. *Stroke* 40(12):e694–e702.
4. Lowery JW, de Caestecker MP (2010) BMP signaling in vascular development and disease. *Cytokine Growth Factor Rev* 21(4):287–298.
5. Bray SJ (2006) Notch signalling: A simple pathway becomes complex. *Nat Rev Mol Cell Biol* 7(9):678–689.
6. Johnson DW, et al. (1996) Mutations in the activin receptor-like kinase 1 gene in hereditary haemorrhagic telangiectasia type 2. *Nat Genet* 13(2):189–195.
7. Urness LD, Sorensen LK, Li DY (2000) Arteriovenous malformations in mice lacking activin receptor-like kinase-1. *Nat Genet* 26(3):328–331.
8. McAllister KA, et al. (1994) Endoglin, a TGF-beta binding protein of endothelial cells, is the gene for hereditary haemorrhagic telangiectasia type 1. *Nat Genet* 8(4):345–351.
9. Li DY, et al. (1999) Defective angiogenesis in mice lacking endoglin. *Science* 284(5419): 1534–1537.
10. Murphy PA, et al. (2008) Endothelial Notch4 signaling induces hallmarks of brain arteriovenous malformations in mice. *Proc Natl Acad Sci USA* 105(31):10901–10906.
11. Murphy PA, et al. (2012) Notch4 normalization reduces blood vessel size in arteriovenous malformations. *Sci Transl Med* 4(117):ra8.
12. Yao Y, Zebboudj AF, Shao E, Perez M, Boström K (2006) Regulation of bone morphogenetic protein-4 by matrix GLA protein in vascular endothelial cells involves activin-like kinase receptor 1. *J Biol Chem* 281(45):33921–33930.
13. Yao Y, Jumabay M, Wang A, Boström KI (2011) Matrix Gla protein deficiency causes arteriovenous malformations in mice. *J Clin Invest* 121(8):2993–3004.
14. Yao Y, Shahbazian A, Boström KI (2008) Proline and gamma-carboxylated glutamate residues in matrix Gla protein are critical for binding of bone morphogenetic protein-4. *Circ Res* 102(9):1065–1074.
15. Zebboudj AF, Imura M, Boström K (2002) Matrix GLA protein, a regulatory protein for bone morphogenetic protein-2. *J Biol Chem* 277(6):4388–4394.
16. Yao Y, Nowak S, Yochelis A, Garfinkel A, Boström KI (2007) Matrix GLA protein, an inhibitory morphogen in pulmonary vascular development. *J Biol Chem* 282(41): 30131–30142.
17. Boström KI, Jumabay M, Matveyenko A, Nicholas SB, Yao Y (2011) Activation of vascular bone morphogenetic protein signaling in diabetes mellitus. *Circ Res* 108(4): 446–457.
18. Larrivée B, et al. (2012) ALK1 signaling inhibits angiogenesis by cooperating with the Notch pathway. *Dev Cell* 22(3):489–500.
19. Swift MR, Weinstein BM (2009) Arterial-venous specification during development. *Circ Res* 104(5):576–588.
20. David L, Mallet C, Mazerbourg S, Feige JJ, Bailly S (2007) Identification of BMP9 and BMP10 as functional activators of the orphan activin receptor-like kinase 1 (ALK1) in endothelial cells. *Blood* 109(5):1953–1961.
21. Uyttendaele H, Ho J, Rossant J, Kitajewski J (2001) Vascular patterning defects associated with expression of activated Notch4 in embryonic endothelium. *Proc Natl Acad Sci USA* 98(10):5643–5648.
22. Krebs LT, et al. (2004) Haploinsufficient lethality and formation of arteriovenous malformations in Notch pathway mutants. *Genes Dev* 18(20):2469–2473.
23. Lawson ND, et al. (2001) Notch signaling is required for arterial-venous differentiation during embryonic vascular development. *Development* 128(19):3675–3683.
24. Park SO, et al. (2009) Real-time imaging of de novo arteriovenous malformation in a mouse model of hereditary hemorrhagic telangiectasia. *J Clin Invest* 119(11):3487–3496.
25. Al-Shahi R, Warlow C (2001) A systematic review of the frequency and prognosis of arteriovenous malformations of the brain in adults. *Brain* 124(Pt 10):1900–1926.
26. Shao ES, Lin L, Yao Y, Boström KI (2009) Expression of vascular endothelial growth factor is coordinately regulated by the activin-like kinase receptors 1 and 5 in endothelial cells. *Blood* 114(10):2197–2206.
27. Koo BK, et al. (2005) Mind bomb 1 is essential for generating functional Notch ligands to activate Notch. *Development* 132(15):3459–3470.
28. Fischer A, Schumacher N, Maier M, Sendtner M, Gessler M (2004) The Notch target genes Hey1 and Hey2 are required for embryonic vascular development. *Genes Dev* 18(8):901–911.
29. Gerety SS, Wang HU, Chen ZF, Anderson DJ (1999) Symmetrical mutant phenotypes of the receptor EphB4 and its specific transmembrane ligand ephrin-B2 in cardiovascular development. *Mol Cell* 4(3):403–414.
30. Adams RH, et al. (1999) Roles of ephrinB ligands and EphB receptors in cardiovascular development: Demarcation of arterial/venous domains, vascular morphogenesis, and sprouting angiogenesis. *Genes Dev* 13(3):295–306.
31. Palaniswamy C, Sekhri A, Aronow WS, Kalra A, Peterson SJ (2011) Association of warfarin use with valvular and vascular calcification: A review. *Clin Cardiol* 34(2): 74–81.
32. Speer MY, et al. (2009) Smooth muscle cells give rise to osteochondrogenic precursors and chondrocytes in calcifying arteries. *Circ Res* 104(6):733–741.
33. Xue Y, et al. (1999) Embryonic lethality and vascular defects in mice lacking the Notch ligand Jagged1. *Hum Mol Genet* 8(5):723–730.
34. Casey LM, et al. (2006) Jag2-Notch1 signaling regulates oral epithelial differentiation and palate development. *Dev Dyn* 235(7):1830–1844.
35. Yao Y, et al. (2012) Crossveinless 2 regulates bone morphogenetic protein 9 in human and mouse vascular endothelium. *Blood* 119(21):5037–5047.
36. Jumabay M, et al. (2012) Endothelial differentiation in multipotent cells derived from mouse and human white mature adipocytes. *J Mol Cell Cardiol* 53(6):790–800.
37. Yao Y, et al. (2013) A role for the endothelium in vascular calcification. *Circ Res* 113(5): 495–504.